Final Draft
of the original manuscript:

Dry sliding wear behaviour of plasma electrolytic oxidation coated AZ91 cast magnesium alloy

P. Bala Srinivasan[*], C. Blawert, W. Dietzel
Institute of Materials Research
GKSS-Forschungszentrum Geesthacht GmbH
D21502 Geesthacht, Germany

*Corresponding Author (bala.srinivasan@gkss.de)
Phone: 00-49-4152-871997; Fax: 00-49-4152-871909

Abstract

A cast AZ91 magnesium alloy was plasma electrolytic oxidation (PEO) coated using a pulsed unipolar power source in a silicate based electrolyte. Constant processing conditions for two different durations were chosen to obtain coatings of 10 μm and 20μm thickness. The dry sliding wear studies performed on this alloy with and without PEO coatings against an AISI 52100 steel ball counterpart showed that the PEO coating improved the wear resistance. The thickness of the PEO coating was found to be highly influential in imparting the wear resistance to this alloy, especially in conditions involving higher contact stresses.

Key words

Magnesium alloy; plasma electrolytic oxidation; microstructure, wear resistance;

Introduction

Magnesium alloys combining good mechanical properties and light weight are an attraction to the automotive and aerospace sectors [1]. For most of the applications the components require a modification to the surface as magnesium alloys exhibit a poor corrosion and wear resistance [2-3]. A wide range of surface treatments are applied to combat the above issues [3-4]. The plasma electrolytic oxidation (PEO) has been found to be very promising for imparting a superior corrosion resistance [5-7]. Even though the PEO coatings have been reported to improve the tribological behaviour of magnesium alloys, the published information is very limited [8-9]. The current work is an

attempt to understand the dry sliding wear behaviour of a cast AZ91 magnesium alloy with and without PEO coatings on the surface.

Experimental

AZ91 magnesium alloy specimens of size 25 mm x 40 mm x 5 mm were used in this investigation. The specimens were polished to 2500 grit emery finish, and were subjected to PEO treatment in a silicate based electrolyte containing 10 g sodium silicate and 10 g potassium hydroxide in 1 liter of double distilled water. The PEO treatment was carried out for 10 and 30 minutes using a pulsed unipolar source with the following process parameters: current density 25 mA·cm^{-2}; pulse width 2 ms; on/off pulse ratio 1:10; temperature: 10 $\pm$ 2°C. The coating morphology was observed in a Cambridge scanning electron microscope. The phase composition analysis was done in a Bruker XRD system with Cu-Kα radiation. The dry sliding wear behaviour of the untreated and PEO coated specimens was assessed using a Tribotec ball on disc oscillating tribometer with an AISI 52100 steel ball of 6 mm diameter as static friction partner. The wear tests were performed at ambient conditions (25 $\pm$ 2°C, 30 $\pm$ 2% RH) at three different load levels, viz., 2N, 5N and 10N with an oscillating amplitude of 10 mm and at a sliding velocity of 5 mm s^{-1} for a sliding distance of 12 m. Surface roughness and wear depth measurements were performed with a Hommel profilometer, and thickness was assessed using Mini Test 2100 coating thickness meter. The worn ball surfaces were examined in a Leitz optical microscope. Characterisation of the wear tracks and the wear debris was done in SEM with energy dispersive spectra (EDS) analysis facility.

Results and Discussion

Figures 1(a) and (b) and **2(a) and (b)** show the cross-section and surface morphology of the PEO coated specimens A and B, treated for 10 and 30 minutes, respectively.

Both specimens showed the presence of pores, characteristic of PEO coating. However, the pore sizes were apparently larger in specimen B, on account of higher voltages and consequent larger spark sizes during the PEO processing. The thickness measurements with Mini Test 2100 showed that the 10 minutes treatment resulted in a coating thickness of 10 ± 1 µm and the 30 minutes treatment yielded 19 ± 2 µm. The SEM images showing the cross-section of specimens A and B (Figures 1(a) and 2(a), corroborate the above data. The voltage vs. time measurements revealed that the increase in voltage was rapid in the initial stages, reaching 400 V in 3 minutes, slowing down from that point onwards to final voltages of 422 ± 2 V and 443 ± 2 V for specimens A and B, respectively. Surface roughness measurements revealed a mean surface roughness (R_a) value of 0.6 – 0.7 µm for the PEO coated specimen A, and 1.1 – 1.2 µm for specimen B. This suggests that the higher processing voltage is not only responsible for the development of a thicker film, but the associated larger spark sizes also influence the surface roughness in a detrimental way.

The dry sliding wear behaviour of the AZ91 alloy shown in **Figure 3a** reveals that the friction coefficient values were fluctuating in the range of 0.24 – 0.40 for the parent alloy, almost independent of different loads of testing. However, the average friction coefficient values for the 2N, 5N and 10N cases were 0.31, 0.28 and 0.27, respectively. In the case of PEO coated specimen A, a different behaviour was observed. In the test at 2N, the friction coefficient was observed to increase steadily, before reaching a steady state value of around 0.78 + 0.02 after approximately 4 m of sliding **(Figure 3b)**. In the case of the test at 5N, a similar increase in the friction coefficient value was observed; however, the value dropped to around 0.35 after a sliding distance of approximately 5 m. In the 10N test, the drop in friction coefficient value was noticed in a very short time, viz., in less than 0.5 m of sliding. The wear behaviour of the PEO coated specimen B with a higher coating thickness was distinctly different from that of

the other two (Figure 3c). At all the loads, no drop in friction coefficient was observed; however, the steady state friction coefficient values were different for the three loads, and with an increase in load a lower value was registered (~0.8 at 2N, ~0.68 at 5N and ~0.62 at 10N). Further, the running-in period was quicker in the test at higher loads. XRD measurements revealed that the PEO coating was constituted by MgO, Mg_2SiO_4 and $MgAl_2O_4$, and it is not surprising that the friction coefficient values were different for the untreated magnesium-steel ball and PEO coated AZ91- steel ball sliding couples.

The micrographs of the wear tracks of the untreated and PEO coated magnesium alloy specimens, examined in SEM, are presented in Figure 4. The extent of damage in the untreated (UT) specimen under different loads is evident in the micrographs, and the wear track widths were found to be higher for the higher test loads. Even though the metal-to-metal contact between the steel ball and magnesium substrate was expected to result only in adhesive wear, it appears to have resulted in a combination of adhesive and abrasive wear. The hardness of the steel ball was approximately 900 HV and that of the magnesium substrate was only around 85 HV. The sliding of the steel ball with a high contact stress in the initial stages (with a point contact) results in the wear of magnesium substrate and the consequent transfer of this material to the ball by adhesive transfer. Upon further continuous sliding, the material transferred to the ball surface got work hardened due to the extensive plastic deformation. It is also probable that the transferred material might have oxidized during sliding and hence the deep grooves observed in the wear tracks could be due to the materials transferred onto the ball. Also, the ß-phase particles removed from the substrate due to wear could have contributed to scoring marks as a three body wear. Mondal et al., [10] described the wear of ACM720 magnesium alloy to be completely abrasive in nature when slid against EN32 steel. However, in the current work the wear debris from the magnesium substrate did not get removed as particles as one would expect in abrasive wear.

Instead, they formed as ridges along the sides of the grooves and also got transferred to the ball. It has to be pointed out here that there was no perceptible wear of the steel ball slid against the magnesium substrate. The worn out balls were examined in optical microscope and the surface appearances are shown in **Figure 5**. Adhesive transfer of material from the magnesium substrate to the steel ball can be noticed in the balls slid against the untreated specimen (UT) and the increased levels of metal pick-up at higher test loads is also evident.

The diameter of worn region of the steel ball slid against the PEO coated specimen A at 2N was around 650 µm. The ball slid against the untreated specimen under similar test conditions also had a more or less similar wear scar dimensions. However, the surface appearances of these two balls were distinctly different as could be seen from Figure 5 (UT-2N, A-2N). On one hand, the ball tested against untreated magnesium substrate revealed an adhesive transfer of material but on the other hand, the ball slid against PEO specimen A seems to suffer from wear damage due to sliding against hard ceramic coating. Scoring marks and the flattened surface seen on the ball suggest that the wear could be abrasive due to the rubbing against the rough ceramic layer as the hardness of the PEO coatings in general has been reported to be around 350 – 600 HV [11], and Liang et al., have reported a value of around 520 HV for a silicate based PEO coating [12]. A closer examination of the wear track of the PEO coated specimen (Figure-A2N) revealed that the PEO layer was more or less intact. Even though a couple of scratches were seen along the sliding direction on the surface, the coating seems to have provided the resistance to the magnesium substrate against adhesive wear.

In the tests at 5N and 10N, the PEO coating in specimen A was found to have failed completely. The drop in the friction coefficient values observed in the tests at 5N and

10N (Figure 3b) can be attributed to the failure and complete removal of PEO coating from the surface. The consequent establishment of metal-to-metal contact had resulted in adhesive transfer from the magnesium substrate to the steel ball. The wear tracks of these two specimens (Figure 4-A5N, A10N) looked very similar to those observed in the case of untreated magnesium substrate, showing extensive wear damage. Coating thickness of around 10 µm in specimen A was apparently insufficient to resist the load of even 5N, and it appears that the Hertzian contact stress under these conditions was high enough to make the coating to crumble, thus causing the complete removal of the coating during sliding. Studies using a profilometer suggested that the PEO coated specimen A tested at 5N and 10N had wear scar depths of 18 µm and 28 µm, respectively.

The surface of the steel balls tested against specimen B had some scoring marks under all loads and the diameters of the worn surfaces of the balls were larger compared to the other two cases (slid against untreated and PEO specimen A). The wear rates of the balls that were run against the untreated and PEO coated specimen A could not be calculated as it was very difficult to measure the "true" dimension of the wear scar on the respective balls. However, the normalized wear rates of the balls that slid against the thick PEO specimen B at 2N, 5N and 10N were calculated to be 1.6442×10^{-4}, 1.433×10^{-4} and 1.3762×10^{-4} mm³/N/m, respectively. The discoloration of the steel balls, especially those tested against the specimen B at 5N and 10N, indicates the possibility of oxidation of this surface during sliding. This further suggests that the wear mechanism in these cases could be a combination of abrasive and oxidative wear. As mentioned earlier, lower friction coefficient values were registered at higher test loads for the PEO specimen B. It is plausible that the debris generated due to oxidative wear under these higher loads could have contributed to the reduction in friction coefficient values as well as some leveling effects removing the highest points of the PEO

coatings. This indicates clearly that even though the wear scar on the balls tested at higher loads looks larger, their normalized wear rates still remain low.

The appearance of the corresponding wear tracks on the PEO coated specimen B (Figure 4 – B2N, B5N and B10N) was different from that of the specimen A at all the three test loads, indicating that this surface has a much higher resistance to adhesive wear. Even though the phase composition of the PEO coating was the same in both the specimens (A&B), the differences in the thickness of the coatings seems to have played a crucial role in the wear process. The wear depths in the PEO specimen B tested at 2N, 5N and 10N were 1 μm, 4 μm and 5 μm respectively. This demonstrates that the coating was not completely removed in PEO coated specimen B under all test conditions.

The normalized wear rates of the untreated and PEO coated specimens under different loads **(Figure 6)** were observed to increase with increase in load from 2N to 5N, in all the three surface conditions. However, a lower wear loss was noticed in the tests at 10N.   Also, it is interesting to note that the wear loss of the specimen B was 10 times lower than that of specimen A at 5N and 10N loads. As discussed earlier, the thicker coating in specimen B has provided a superior wear resistance and it is pertinent to point out that the wear tests started with a high stress level, with a point contact, and as the wear process goes on, the contact stress came down to lower values. At higher stress levels, the deformation of the substrate under loading/sliding caused the cracking and flaking of thin coatings. Under these circumstances the increased thickness provided a better load bearing capacity and thus offered a better wear resistance.

The regions marked in squares in the wear tracks of the specimens A and B in Figure 4 were examined at higher magnifications to understand extent of damage and the wear

mechanism. Scanning electron micrographs of the wear tracks of specimen A tested at 2N, 5N and 10N are shown in **Figures 7(a), (b) and (c)**, respectively. This specimen tested at 2N had shown a wear rate of 4.2 x 10^{-4} mm³ N^{-1} m^{-1}, with a corresponding wear depth of around 3 µm. In Figure 7(a), loose wear debris can be noticed on the wear track and the PEO coating was seen underneath the debris, revealing that a major part of the PEO coating was still intact. Under 5N and 10N, the coating was completely removed. This has resulted in the establishment of contact between the magnesium substrate and the steel ball, and thus developed scoring marks on the magnesium surface as can be seen in Figures 7(b) and (c). In the tests at higher loads, the coating had apparently cracked in the regions adjoining the wear track and large parts of flaked-off regions are visible along the edges of these wear tracks.

In the case of the PEO coated specimen B tested at 2N, the appearance of the wear track **(Figure 8(a))** was more or less similar to that observed in the case of specimen A. Even though the normalized wear rates presented in Figure 5 suggest a much lower wear loss for the specimen B when compared to the other two specimens, the wear tracks of this specimen appear to contain a relatively higher quantity of wear debris. Further, some of the protruding surface seems to have got leveled out during sliding. The higher quantity of wear debris seen was on account of the wear of the ball in addition to the wear of the PEO layer. The appearances of the wear tracks produced at 5N and 10N in specimens A and B were distinctly different **(Figures 8(b) and (c))**. While the PEO coating was completely removed in specimen A at 5N and 10N and the magnesium substrate was found to undergo a combined adhesive–abrasive wear damage, the wear tracks of specimen B at these two loads contained loose wear debris as was observed in the case of the test at 2N. Further, it looks as if the wear debris got smeared on the surface, filling the pores under the combined action of load and sliding. As mentioned earlier, the profilometry studies on these wear tracks showed wear

depths of 4 μm and 5 μm at 5N and 10N, respectively. Despite the removal of small amounts material, the coating appeared to be more or less intact, may be only pressed into the substrate, and no catastrophic wear failure occurred under any of the three test conditions employed in this investigation.

The scanning electron micrograph of the wear track of the PEO coated specimen A tested at 10N is shown in **Figure 9(a)** and the EDS analysis from the region marked in this micrograph is presented in **Figure 9(b)**. As was mentioned earlier, the PEO coating was completely removed from the surface during this test, and there is no surprise that the EDS analysis showed predominantly magnesium and aluminium with small amounts of oxygen. The scanning electron micrograph of the wear track of the PEO coated specimen B tested at 10N is shown in **Figure 10(a)**. It is evident that the debris consists of very fine sized particles and the EDS analysis performed in the marked region shows high intensity peaks of O, Fe, Mg, Si and Al **(Figure 10(b)**. This confirms that the abrasive/oxidative wear of steel ball was very much present in the wear process involving steel ball-PEO coated surface, in addition to the mild wear of the PEO coating.

As a whole, this investigation brings out the fact that the thickness of the PEO coating is very critical in resisting adhesive wear damage of the magnesium substrate, especially at higher contact stress levels. Further studies are planned to determine the failure and the detailed wear mechanisms (under dry and lubricated sliding conditions) of the coatings as a function of coating thickness by interrupting the wear tests at different points of time.

Conclusions

In summary, the friction coefficient values for the PEO-steel ball sliding couple are much higher than that for the magnesium substrate-steel ball under different loads. The wear

resistance of the AZ91 magnesium alloy is significantly improved by PEO coatings on the surface, and the thickness of the coating plays a crucial role in enhancing the wear resistance still further. At higher initial stress levels, the deformation of the substrate causes the cracking and flaking-off of the coating, especially when it is thin. Under such circumstances the increased thickness of PEO coating provides a better load bearing capacity, thus resulting in a superior wear resistance. The appreciable reduction in the wear rates of the PEO coated substrate with higher thickness is at the expense of some minor abrasive wear of the steel ball. The damage of the steel ball, quantified as specific wear rate, was found to be influenced by the test load and wear mechanisms involved. Oxidation of the steel ball surface, especially under higher test loads seems to be beneficial in bringing down the friction coefficient and specific wear rates, as well.

Acknowledgement

References

1. H. Westengen, Light Metal Age, 58 (2000) 44–52.

2. G. Song, A. Atrens, Advanced Engineering Materials, 5 (2003) 837–858.

3. J.D. Gray, B. Luan: Journal of of Alloys and Compounds, 336 (2002) 88–113.

4. C. Blawert, W. Dietzel, E. Ghali, G. Song, Advanced Engineering Materials, 8 (2006) 511–533.

5. H.F. Guo, M.Z. An, Applied Surface Science, 246 (2005) 229–238.

6. Q. Cai, L.Wang, B. Wei, Q. Liu: Surface and Coatings Technology, 200 (2006) 3727–3733.

7. C. Blawert , V. Heitmann, W. Dietzel, H.M. Nykyforchyn , M.D. Klapkiv, Surface and Coatings Technology, 201 (2007) 8709–8714.

8. J. Liang, B. Guo, J. Tian, H. Liu, J. Zhou, T. Xu, Applied Surface Science, 252 (2005) 345–351.

9. Y. Ma, X. Nie, D.O. Northwood, H. Hu, Thin Solid Films, 469-470 (2004) 472– 477.

10. A.K. Mondal, S. Kumar, C. Blawert, N.B. Dahotre, Surface and Coatings Technology, 202 (2008) 3187–3198.

11. Homepage of Keronite International Ltd at http://www.keronite.com

12. J. Liang, L. Hz, J. Hao, Applied Surface Science, 253 (2007) 4490 – 4496.

Figure Captions

Figure 1   Scanning electron micrographs of the PEO coated specimen A
            (a) Cross-section   (b) Surface morphology

Figure 2   Scanning electron micrographs of the PEO coated specimen B
            (a) Cross-section   (b) Surface morphology

Figure 3   Friction coeffient data from the dry sliding wear tests
            (a) Untreated (b) PEO coated specimen A (c) PEO coated specimen B

Figure 4   Scanning electron micrographs showing the wear tracks in the untreated
            (UT) and PEO coated specimens (A&B)

Figure 5   Optical micrographs showing the surface of wear out steel balls slid
            against the untreated (UT) and PEO coated specimens (A&B)

Figure 6   Wear rate of untreated and PEO coated specimens under different loads

Figure 7   Higher magnification scanning electron micrographs showing the features
            of wear track and the adjoining region in specimen A tested at different
            loads

Figure 8   Higher magnification scanning electron micrographs showing the features
            of wear track and the adjoining region in specimen B tested at different
            loads

Figure 9   SEM-EDS analysis of the wear track in PEO coated specimen A (A-10N)
            (a) micrograph showing the region of EDS analysis   (b) EDS spectra

Figure 10   SEM-EDS analysis of the wear track in PEO coated specimen B (B-10N)
            (a) micrograph showing the region of EDS analysis   (b) EDS spectra
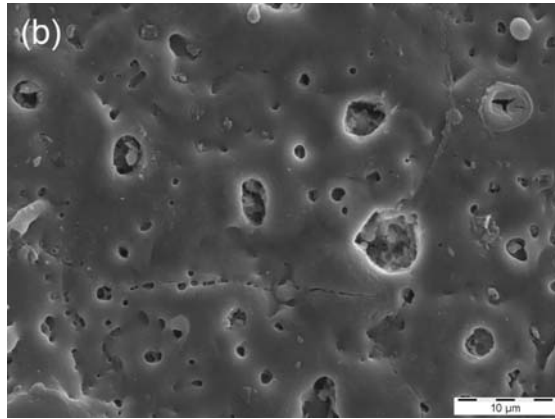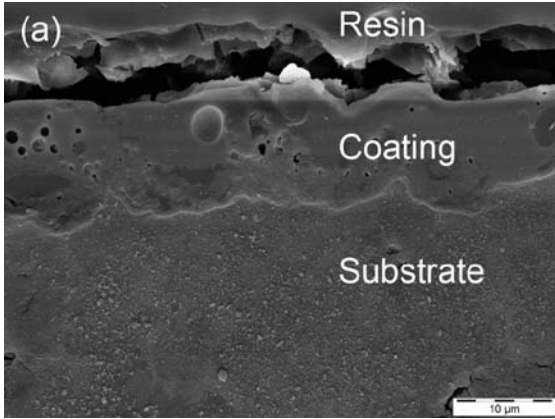
(a) Cross-section   (b) Surface morphology
Figure 1 Scanning electron micrographs of the PEO coated specimen A (10 minutes)
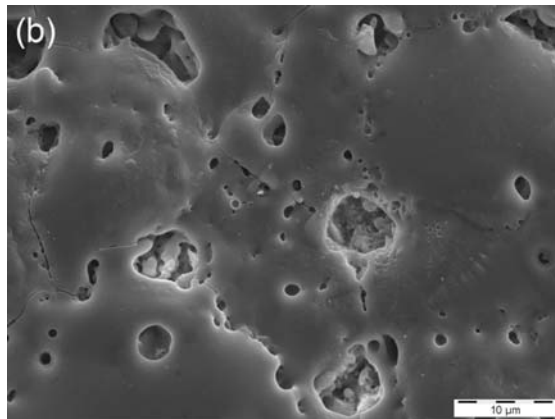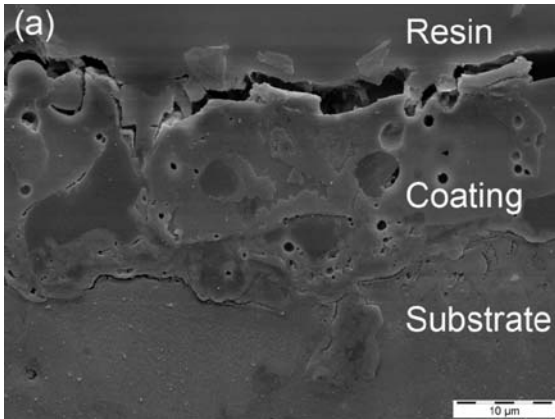
(a) Cross-section   (b) Surface morphology
Figure 2 Scanning electron micrographs of the PEO coated specimen B (30 minutes)
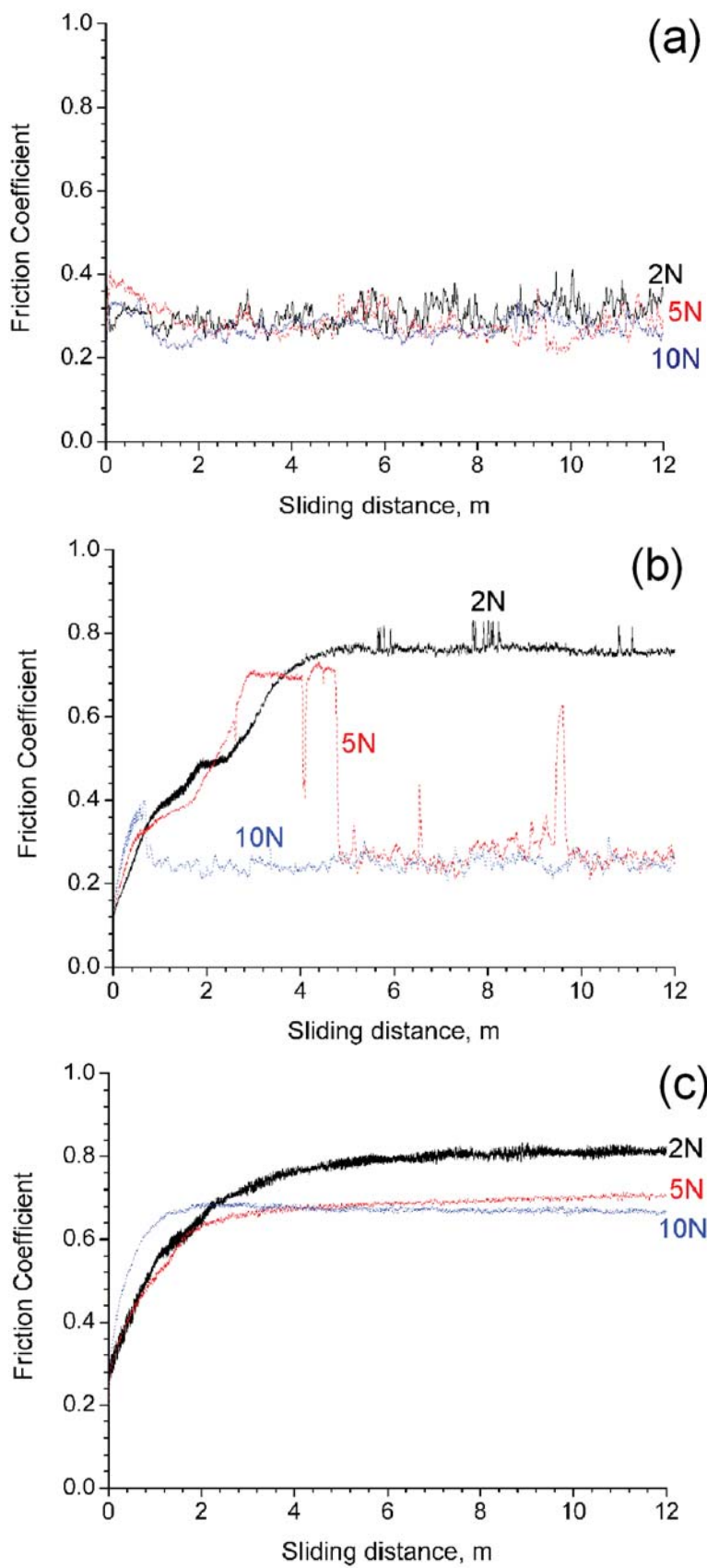
Figure 3 Friction coeffient data from the dry sliding wear tests: (a) Untreated, (b) PEO coated specimen A, (c) PEO coated specimen B.
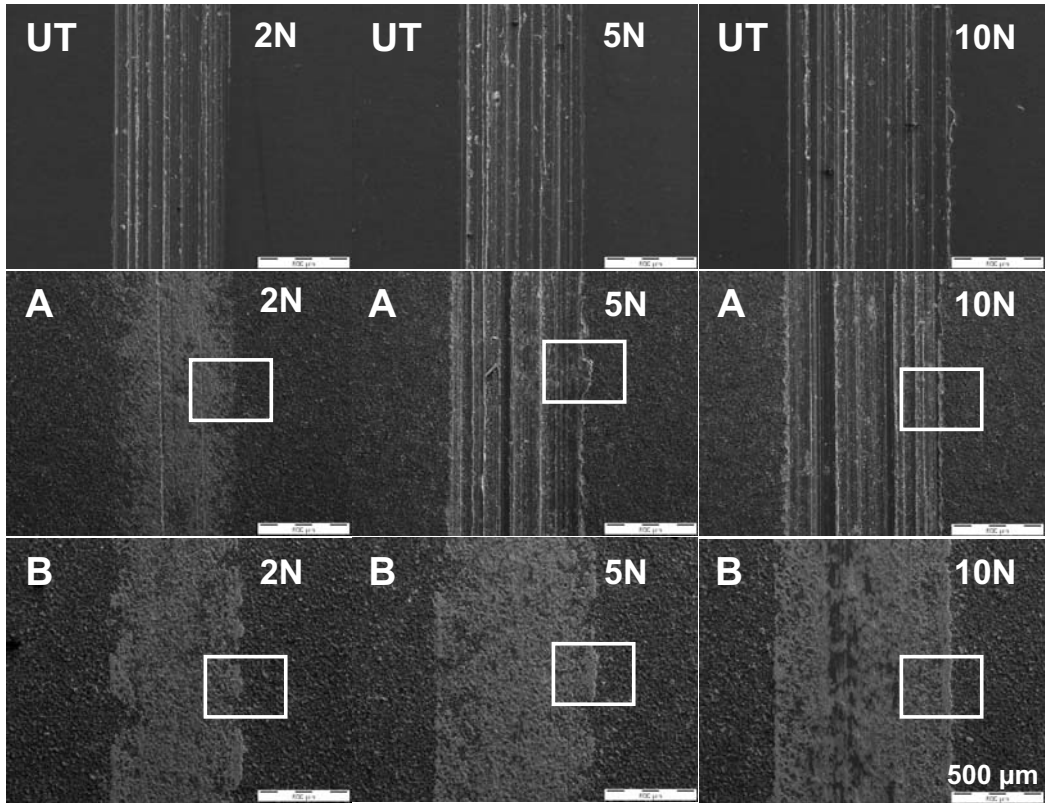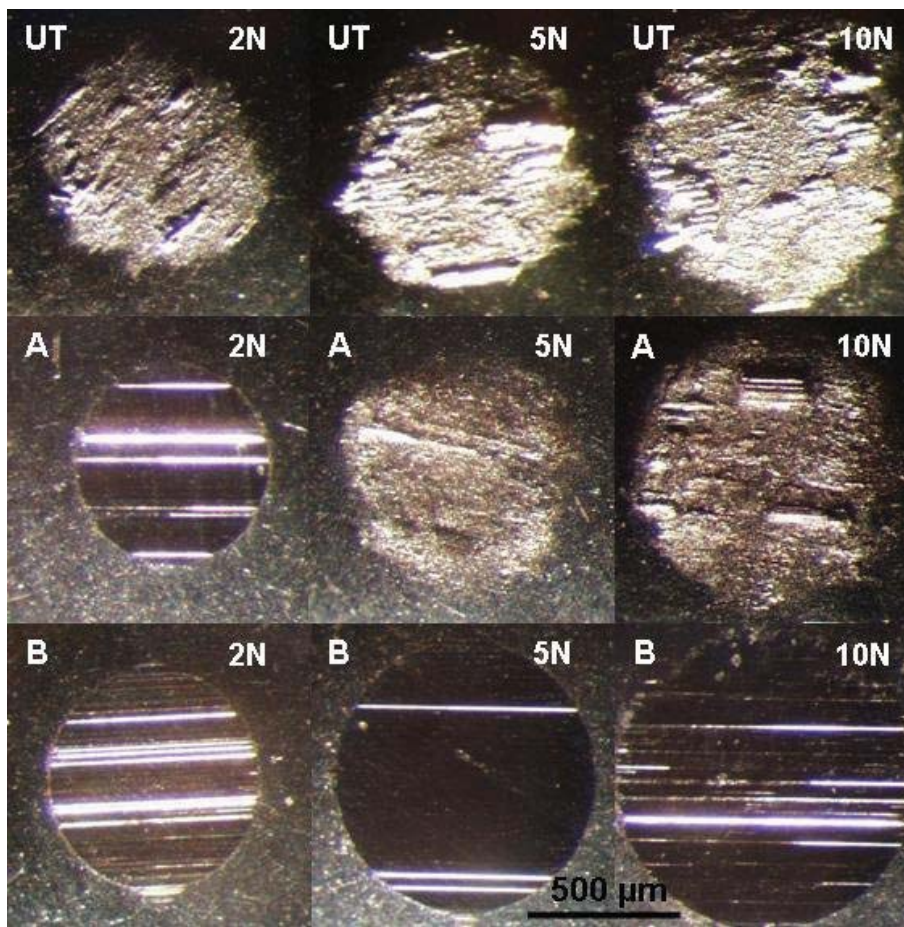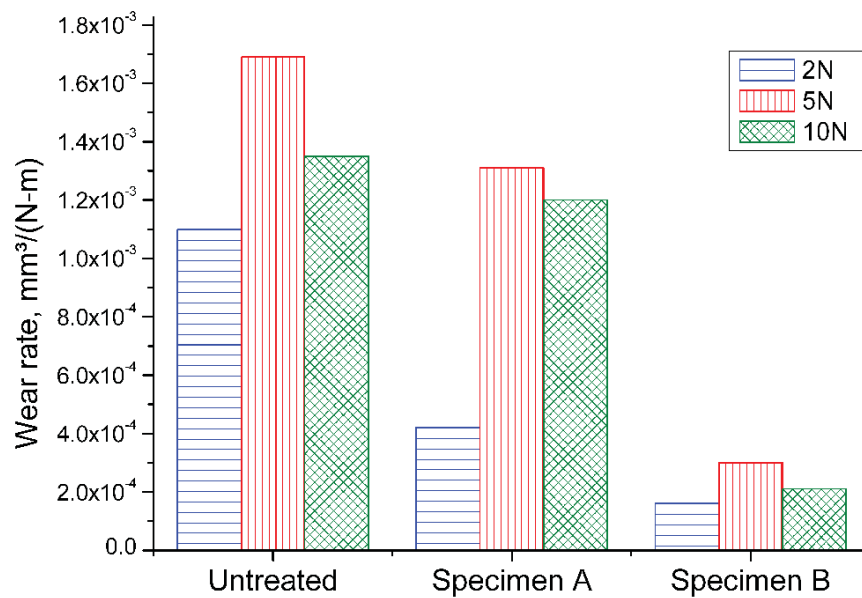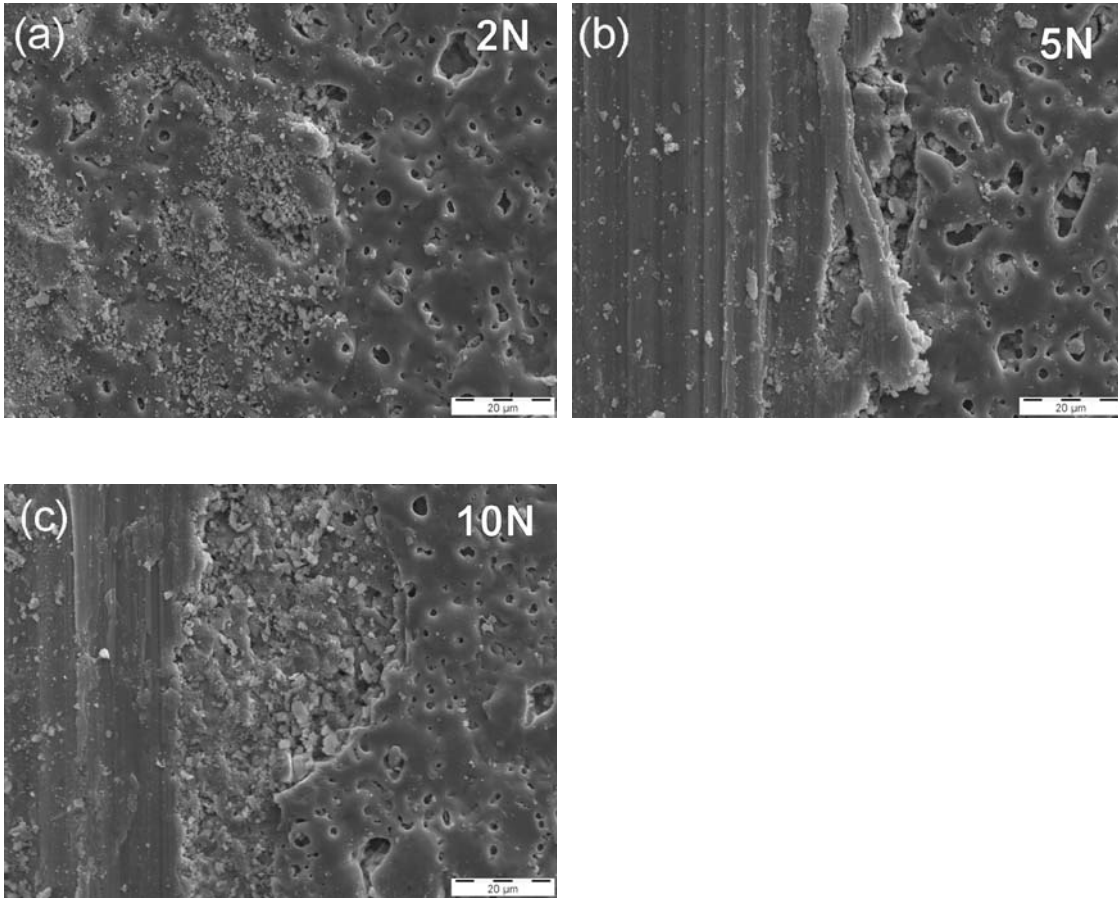
Figure 4 Scanning electron micrographs showing the wear tracks in the untreated (UT) and PEO coated specimens (A&B) (Regions marked in squares are discussed in the later section)

Figure 5 Optical micrographs showing the surface of wear out steel balls slid against the untreated (UT) and PEO coated specimens (A&B)

Figure 6 Wear rates of untreated and PEO coated specimens under different loads

Figure 7 Higher magnification scanning electron micrographs showing the features of wear track and the adjoining region in specimen A tested at different loads
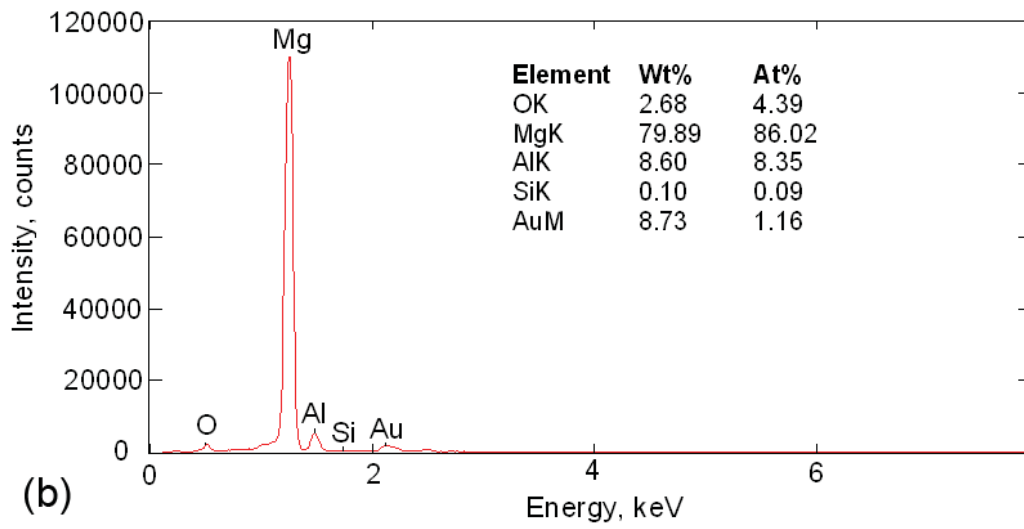
Figure 8 Higher magnification scanning electron micrographs showing the features of wear track and the adjoining region in specimen B tested at different loads
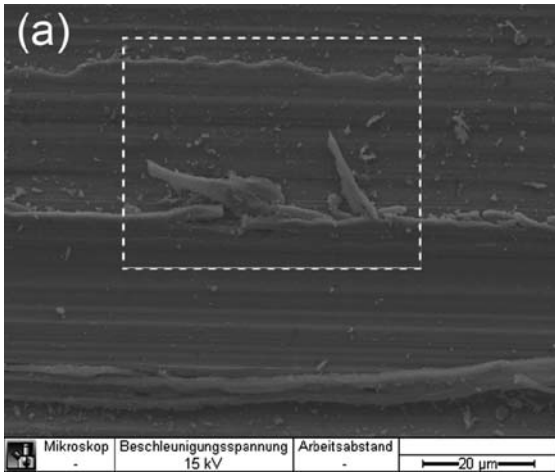
Figure 9 SEM-EDS analysis of the wear track in PEO coated specimen A (A-10N)
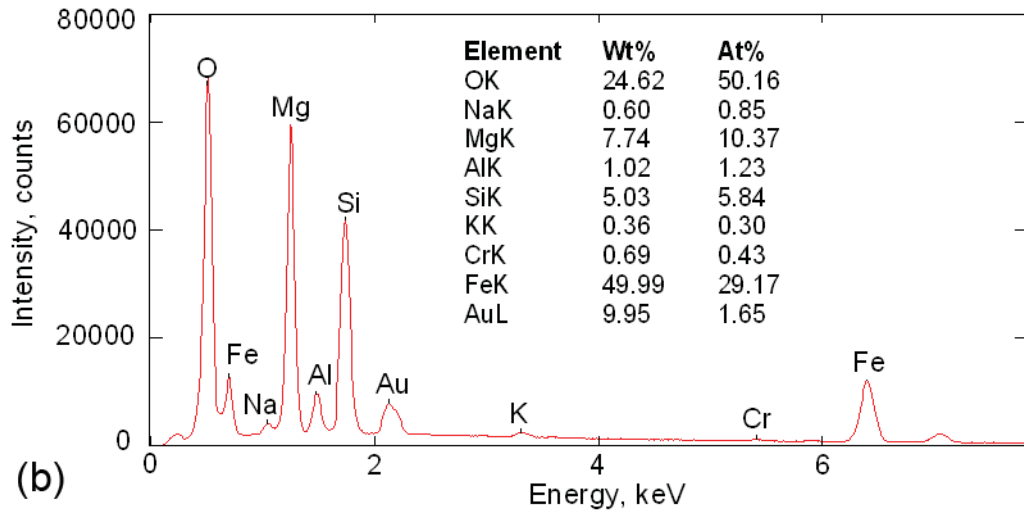(a) micrograph showing the region of EDS analysis   (b) EDS spectra
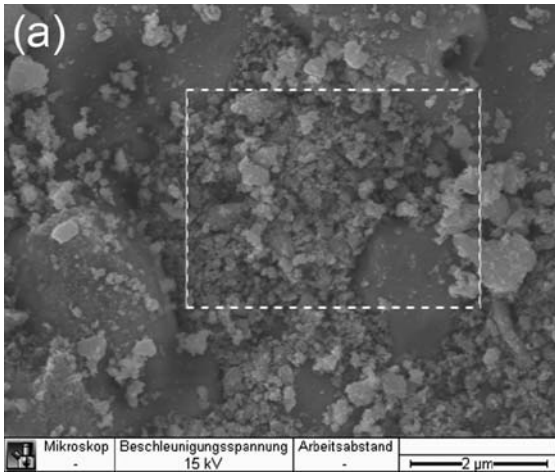
Figure 10 SEM-EDS analysis of the wear track in PEO coated specimen B (B-10N)
(a) micrograph showing the region of EDS analysis   (b) EDS spectra